ISSN 1063-7761, Journal of Experimental and Theoretical Physics, 2014, Vol. 119, No. 5, pp. 817–827. © Pleiades Publishing, Inc., 2014.
Original Russian Text © V.E. Zobov, 2014, published in Zhurnal Eksperimental'noi i Teoreticheskoi Fiziki, 2014, Vol. 146, No. 5, pp. 933–945.

ATOMS, MOLECULES, OPTICS

Quantum and Classical Correlations in Electron–Nuclear Spin Echo

V. E. Zobov

Kirensky Institute of Physics, Siberian Branch, Russian Academy of Sciences, Akademgorodok, Krasnoyarsk, 660036 Russia
e-mail: rsa@iph.krasn.ru

Received June 5, 2014

Abstract—The quantum properties of dynamic correlations in a system of an electron spin surrounded by nuclear spins under the conditions of free induction decay and electron spin echo have been studied. Analytical results for the time evolution of mutual information, classical part of correlations, and quantum part characterized by quantum discord have been obtained within the central-spin model in the high-temperature approximation. The same formulas describe discord in both free induction decay and spin echo although the time and magnetic field dependences are different because of difference in the parameters entering into the formulas. Changes in discord in the presence of the nuclear polarization β_I in addition to the electron polarization β_S have been calculated. It has been shown that the method of reduction of the density matrix to a two-spin electron–nuclear system provides a qualitatively correct description of pair correlations playing the main role at $\beta_S \approx \beta_I$ and small times. At large times, such correlations decay and multispin correlations ensuring nonzero mutual information and zero quantum discord become dominant.

DOI: 10.1134/S1063776114110132

1. INTRODUCTION

Spin echo discovered by Hahn [1] underlies many applications of magnetic resonance, on one hand, as a method for studying the local properties of solids and fluids [2, 3] and, on the other hand, as an implemented example of the Loschmidt echo when studying nonequilibrium processes in multispin systems [4, 5]. Interest in studying quantum information has been recently grown [6–9], primarily in view of its properties promising fundamentally new possibilities in the speed of a quantum computer for the development of communication and metrology. Because of technical difficulties, real devices implementing these possibilities on multiparticle quantum systems have not yet been developed. However, the physical properties of quantum information can be studied on such systems by traditional methods, including the spin echo method. The system of an electron spin surrounded by nuclear spins is practically important and well-studied by this method. In particular, references to the methods used, results obtained, and their analysis can be found in theoretical works [10–14]. Such a system seems to be also promising for the implementation of quantum information processing devices [15].

The system of the electron spin surrounded by nuclear spins is close in structure to quantum systems used to implement the deterministic quantum calculation model with one polarized qubit interacting with a system of qubits in a mixed state (DQC1) [16]. It is known that the computer of the DQC1 model can theoretically solve some problems reduced to the calculation of the trace of a matrix faster than a classical computer [16–23]. The operation of such a computer was demonstrated on simple systems: e.g., molecules in a solution controlled by the NMR method [18, 20, 23] and Ce^{3+} impurities in a CaF_2 crystal observed by the EPR method [24]. It is assumed that quantum correlations play an important role in the speed of the DQC1 model. Quantum discord [9] is the most popular measure of quantum correlations at high temperatures. In order to reveal the role of quantum correlations, quantum discord in the operation of the DQC1 computer was estimated in [17, 19, 21–23]. However, a certain conclusion has not yet been made [19, 21–23, 25] and the dynamics of such systems requires further investigations.

The time evolution of quantum discord under the conditions of electron spin echo and free-precession decay in the system of an electron surrounded by nuclei is considered in this work. It is shown that the dynamics of such a system is similar to the dynamics of the DQC1 model. These two systems differ in the control methods: in the DQC1 model, each nuclear spin should be controlled individually in order to implement a quantum algorithm, whereas the evolution of nuclear spins in the case of spin echo is caused by the internal interactions and an external magnetic field. Any calculations of discord under the conditions of spin echo are unknown among numerous calculations of discord in various systems. There are several similar works. The time and temperature dependences of discord for two $S = 1/2$ spins were calculated in [26] under the conditions of multiquantum coherence and in [27] under the conditions of free induction decay (FID) of an impurity spin interacting with a chain of nuclear spins. The evolution of quantum correlations between two large spins ($S > 1/2$) under the conditions

of FID was calculated in [28] in the high-temperature approximation. Finally, the authors of [29] prepared a special (Bell) state of an ensemble of two-spin electron–nucleus systems with nonzero discord on a phosphor impurity in solid silicon and observed its decrease under the action of surrounding spins of ^{29}Si nuclei considered as a random field (noise).

Quantum effects were considered in many works concerning spin echo. In particular, the authors of [30, 31] related change in the decay of the electron spin echo of an NV center in diamond with an increase in the magnetic field to attenuation of quantum fluctuations. They think that, if the decay of echo is due to changes in the states of nuclei caused by flip of the electron spin (back action), the action of the system of nuclei should be considered as quantum (quantum reservoir) [30–32]. On the contrary, if changes in the states of nuclei responsible for the damping of echo are independent of the state of the electron spin, this reservoir is treated as classical. For comparison of two characteristics of quantization, quantum discord is calculated in this work under the same conditions.

The paper is organized as follows. Analytical results describing the time evolution of the quantum discord of the spin echo and the FID for the central-spin model are obtained in Section 2 in the high-temperature approximation with allowance for only the polarization of electron spin. The dependence of discord on the number of nuclei and on the magnetic field, as well as its relation to the quantization characteristic of the reservoir of nuclei determined by the back action property, is discussed. The contribution from the polarization of nuclear spins is additionally taken into account in Section 3, where related changes in the time dependence of discord are also analyzed. The calculation is performed for the total density matrix and a matrix reduced to a pair of spins. The results of two approaches are compared. The general conclusions on the dynamics of the system under consideration are summarized in Section 4. The details of the calculations are presented in Appendices A, B, and C.

2. QUANTUM DISCORD IN THE CENTRAL-SPIN MODEL

2.1. Theory

We consider the system of an electron spin and n nuclear spins in a strong static magnetic field described by the Hamiltonian [10–14, 24, 29–31]

$$\hat{H} = \omega_e \hat{S}_e - \sum_j \omega_j \hat{I}_{jz} + \hat{S}_z \sum_j A_{jz} \hat{I}_{jz} + \hat{S}_z \sum_j A_{jy} \hat{I}_{jy} + \hat{S}_z \sum_j A_{jx} \hat{I}_{jx} + \hat{H}_{II}, \quad (1)$$

where ω_e and ω_j are the Larmor frequencies of the electron, $S = 1/2$, and nuclear, $I = 1/2$, spins, respectively; the system of units with $\hbar = 1$ is used; $\hat{I}_{j\alpha}$ is the α component of the jth spin operator ($\alpha = x, y, z$); $A_{j\alpha}$ is the hyperfine coupling constant; and $\hat{H}_{II}$ is the operator of the dipole–dipole interaction between nuclear spins.

The polarization for electron spins in the strong static magnetic field at room temperature T is small, $\beta_S = \omega_e/kT \sim 10^{-3} \ll 1$, and the polarization for nuclear spins β_I is three orders of magnitude smaller; for this reason, the equilibrium density matrix is initially taken in the form [24, 29, 33, 34]

$$\hat{\rho}_{\text{eq}} = (1 - \beta_S \hat{S}_z)/Z, \quad (2)$$

where $Z = 2^{n+1}$ is the partition function. The effect of nuclear polarization will be considered in the next section. The subsequent calculations will be performed in the reference frame rotating with the frequency ω_e (below, rotating reference frame) in which the first Zeeman term in Eq. (1) disappears. An microwave field pulse applied to the system induces the rotation of the electron spin by an angle of 90° about the y axis of the rotating reference frame. After the application of the pulse, an FID signal $g_f(t)$ will be observed in the xy plane. If the system after time t is subjected to the second microwave pulse rotating the electron spin by an angle of 180° about the x axis of the rotating reference frame, the spin echo with the amplitude $g_e(t)$ will be observed at time $2t$. The density matrix describing the evolution of the state of the system can be written in both cases in the form

$$\hat{\rho}(t) = \frac{1}{Z}\left[1 - \frac{\beta_S}{2}\{\hat{S}_+ \hat{U}^+_{(f,e)}(t) + \hat{S}_- \hat{U}^-_{(f,e)}(t)\}\right] = \frac{1}{Z}[1 - \beta_S \Delta\hat{\rho}_{SI}(t)], \quad (3)$$

where $\hat{S}_\pm = \hat{S}_x \pm i\hat{S}_y$;

$$\hat{U}^+_f(t) = \exp(-it\hat{H}_+)\exp(it\hat{H}_-),$$
$$\hat{U}^+_e(t) = \exp(-it\hat{H}_+)\exp(-it\hat{H}_-) \times \exp(it\hat{H}_+)\exp(it\hat{H}_-), \quad (4)$$

$\hat{H}_+$ and $\hat{H}_-$ are Hamiltonian (1) for the projections of the electron spin $S_z = +1/2$ and $-1/2$, respectively; and $\hat{U}^-_{(f,e)}$ is the operator that is Hermitian conjugate to $\hat{U}^+_{(f,e)}$. Similar transformations of evolution operators (4) are often used to describe spin echo in electron–nuclear systems. Details can be found in Appendix A. The FID signal or echo amplitude is obtained from Eq. (3) in the form

$$g_{(f,e)}(t) = \frac{\langle \hat{S}_x(t)\rangle}{\langle \hat{S}_x(0)\rangle} = \frac{\text{Tr}\{\hat{S}_x \hat{S}_x(t)\}}{\text{Tr}\hat{S}_x^2} = \text{ReTr}(\hat{U}^+_{(f,e)}(t)),$$

where $\langle \hat{S}_x(t)\rangle = \text{Tr}\{\hat{S}_x \rho(t)\}$ is the average value of the x projection of the spin.

Density matrix (3) has the same form as the quantum calculation matrix in the DQC1 model [16, 17]. In the latter case, the unitary operator $\hat{U}_n^+$ whose trace should be calculated to solve the problem is prepared instead of unitary operators (4). The real or imaginary part of the desired trace is determined by measuring the average projection $\langle \hat{S}_x \rangle$ or $\langle \hat{S}_y \rangle$ on the x or y axis, respectively. In view of the similarity of these systems, the approach developed in [17, 19, 21–23] for the DQC1 model can be used to analyze quantum correlations in the state described by Eq. (3).

Correlation between two systems is measured by mutual information [8, 9]

$$I(\hat{\rho}) = S(\hat{\rho}_S) + S(\hat{\rho}_I) - S(\hat{\rho}), \tag{5}$$

where $S(\hat{\rho}) = -\mathrm{Tr}\{\hat{\rho}\log_2\hat{\rho}\}$ is the von Neumann entropy and $\hat{\rho}_S = \mathrm{Tr}_I\hat{\rho}$ and $\hat{\rho}_I = \mathrm{Tr}_S\hat{\rho}$ are the reduced density matrices obtained after the calculation of the trace of matrix (3) over the states of the nuclear spins and electron spin, respectively. Classical correlations are determined in terms of mutual information $I(\hat{\Pi}_S(\hat{\rho}))$ of the state after the von Neumann projective measurement of the electron spin [9, 17, 19]. In the case of the system with $S = 1/2$, the complete set of mutually orthogonal projectors consists of two projectors of the general form [9, 17]

$$\hat{\Pi}_{S\pm} = \frac{1}{2} \pm (a_x\hat{S}_x + a_y\hat{S}_y + a_z\hat{S}_z), \tag{6}$$

where a_α ($\alpha = x, y, z$) are the direction cosines. The measure of classical correlations is obtained after the determination of a maximum in the measurement directions. For the state given by Eq. (3), $a_z = 0$, $a_x = \cos\varphi$, and $a_y = \sin\varphi$ are taken following [17]. Quantum discord is defined as the difference of these two quantities [9, 17, 19]

$$D = I(\hat{\rho}) - \max_{a_\alpha} I(\hat{\Pi}_S(\hat{\rho})). \tag{7}$$

For the DQC1 model, it was shown in [17] that discord for a quite complex system with a broad spectrum of the eigenvalues of the operator U_n^+ reaches a certain value that becomes independent of the number of qubits (nuclei) n; in our high-temperature limit, this value is (see Appendix C)

$$D \approx \frac{\beta_S^2}{16\ln 2}. \tag{8}$$

For the DQC1 model, it was shown in [19, 21, 22] that discord determined after the measurement of the second (nuclear) subsystem is zero. It is sufficient to take the eigenstates of the operators $\hat{U}_n^\pm$ ($\hat{U}_{(f,e)}^\pm$ in our case) as a basis on which the state $\hat{\rho}(t)$ is projected.

We note that the discord value calculated by means of orthogonal measurements (6) is an upper bound for discord determined with the use of generalized nonorthogonal positive-operator-valued measurements [9, 19, 22, 35]. In the case of measurements on a two-level system, the difference between these discord values is very small (see, e.g., [35]). Qualitative analysis of the properties of dynamic quantum correlations is of primarily interest; for this reason, a simpler orthogonal measurement will be used following [17, 19–22, 27].

For further, more detailed analysis, model (1) is simplified by setting $A_{jz} = A_{jy} = 0$ and $H_{II} = 0$. In this case, we obtain (see Appendix A)

$$\hat{U}_{(f,e)}^\pm(t) = \prod_j \{U_{j0}^{(f,e)}(t) \pm iI_{jx}U_{jx}^{(f,e)}(t) \pm iI_{jy}U_{jy}^{(f,e)}(t)\}. \tag{9}$$

Omitting the subscript j, the functions entering into Eq. (9) for the FID and spin echo can be represented in the from

$$\begin{aligned} U_0^f(t) &= 1 - 2n_x^2\sin^2\frac{t\Omega}{2}, \\ -U_x^f(t) &= F_x = 2n_x\sin(t\Omega), \\ -U_y^f(t) &= F_y = 4n_xn_z\sin^2\frac{t\Omega}{2}, \\ U_0^e(t) &= 1 - \frac{1}{2}F_y^2, \quad U_x^e(t) = -F_xF_y\frac{n_z}{n_x}, \\ U_y^e(t) &= 2F_y\left(1 - F_y\frac{n_z}{2n_x}\right), \end{aligned} \tag{10}$$

where

$$\Omega^2 = \omega^2 + \frac{A_x^2}{4}, \quad n_x = \frac{A_x}{2\Omega}, \quad n_z = \frac{\omega}{\Omega}.$$

In this model, the FID signal or echo amplitude is represented in the form

$$g_{(f,e)}(t) = \prod_j U_{j0}^{(f,e)}(t). \tag{11}$$

Substituting these functions (omitting the superscripts f and e) into general formulas (5) and (7) and retaining the first nonzero term of the expansion in β_S, we obtain (see Appendix B)

$$I(\rho) = \frac{\beta_S^2}{8\ln 2}[1 - g^2(t)], \tag{12}$$

$$\max_\varphi I(\hat{\Pi}_S(\hat{\rho})) = \max_\varphi\left\{\frac{\beta_S^2}{16\ln 2}[1 - g^2(t) - K\cos(2\varphi)]\right\}, \tag{13}$$

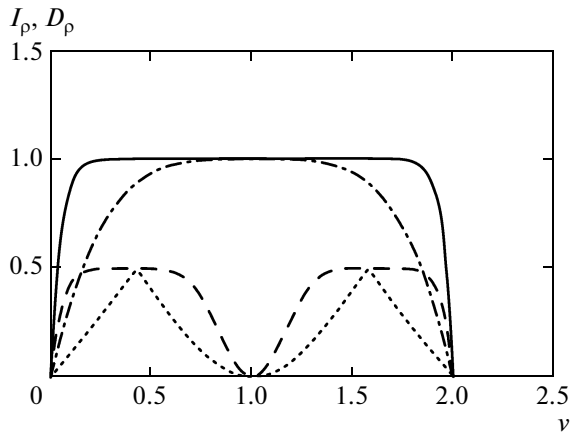

(Solid and dash-dotted lines) Mutual information $I_\rho = I(\rho)8\ln 2/\beta_S^2$ at numbers of nuclei $n = 10$ and 2, respectively, and (dashed and dotted lines) the relative fraction of quantum discord $D_\rho = D/I(\rho)$ at numbers of nuclei $n = 10$ and 2, respectively, versus parameter v (20).

where

$$K = \prod_j U_{j0}^2(t) - \prod_j [2U_{j0}^2(t) - 1]. \quad (14)$$

The maximum in Eq. (13) is reached at $\varphi = 0$ if $K < 0$ and at $\varphi = \pi/2$ if $K > 0$. Therefore, discord (7) can be represented in the form

$$D = \frac{\beta_S^2}{16\ln 2}[1 - g^2(t) - |K|], \quad (15)$$

$$\frac{D}{I(\rho)} = \frac{1}{2}\left[1 - \frac{|K|}{1 - g^2(t)}\right]. \quad (16)$$

Estimate (8) is obtained from Eq. (15) when all products with respect to j are zero. This is the case at quite large times for a fairly large number of nuclei. In this case, $K = 0$ and the dependence on the angle φ disappears in Eq. (13).

To complete this subsection, it is noteworthy that, since mutual information and discord do not change under a unitary transformation of one of two subsystems [9], Eqs. (9)–(16) describe systems with Hamiltonians obtained from Eq. (1) by the rotation of nuclear spin components. For example, if $A_{jx} = A_{jy} = 0$, but $A_{jz} \neq 0$, the nuclear Zeeman interaction has the form $\sum_j \omega_j \hat{I}_{jx}$. In particular, such hyperfine interaction is used to describe phosphor impurities in silicon [11, 29].

2.2. Discussion

To analyze the dependences of Eqs. (12), (15), and (16) on the parameters, we consider a homogeneous case of equal constants $A_{jx} = A$ and Larmor frequencies $\omega_j = \omega$ for n nuclei. In this case,

$$g(t) = U_0^n(t), \quad K = U_0^{2n}(t) - [2U_0^2(t) - 1]^n. \quad (17)$$

Consequently, at even n values,

$$K \geq 0 \quad \text{at} \quad 1/3 \leq U_0^2(t) \leq 1,$$

$$K \leq 0 \quad \text{at} \quad 0 \leq U_0^2(t) \leq 1/3.$$

At odd n values, $K \geq 0$ at any possible $U_0^2(t)$ value. In both cases, discord is maximal at $U_0^2(t) = 1/3$,

$$D = \frac{\beta_S^2}{16\ln 2}[1 - 3^{-m}], \quad (18)$$

where $m = n$ at even n values and $m = n - 1$ at odd n values. In both cases,

$$I(\rho) = \frac{\beta_S^2}{8\ln 2}[1 - 3^{-n}]. \quad (19)$$

The function $U_0^2(t)$ can be represented in the form $U_0^2(t) = (1 - v)^2$, where

$$v = 2n_x^2 \sin^2\frac{t\Omega}{2} \text{ for FID},$$
$$v = 8n_x^2 n_z^2 \sin^4\frac{t\Omega}{2} \text{ for echo}, \quad (20)$$

according to Eqs. (10). In both cases, the parameter v is a periodic function of the time. The magnetic-field dependences of the amplitude of these oscillations are different. With an increase in the magnetic field, this amplitude for the FID decreases from 2 to 0, whereas the amplitude for echo increases first from 0 at $\omega = 0$ to a maximum value of 2 at $\omega = A/2$ and then approaches zero in the limit $\omega \longrightarrow \infty$. The dependences of mutual information (12) and discord (16) on parameter (20) are shown in the figure. They are specified by the same functions of v for both free-precession decay and spin echo.

At $v = 0$, e.g., at the initial time, $U_0^2(t) = 1$ and $D = 0$. We consider the case where $U_0^2(t)$ is close to unity. At $vn \ll 1$, we obtain

$$\frac{D}{I(\rho)} \approx v(n - 1). \quad (21)$$

If $v \ll 1$, but $vn > 1$, the estimate expression follows from Eqs. (12), (16), and (17) in the form

$$\frac{D}{I(\rho)} \approx \frac{1}{2}[1 - \exp(-2vn)], \quad (22)$$

which describes an increase in discord to maximum value (8) at a quite large number of nuclei.

With a further increase in the time to $t\Omega/2 = \pi$, again $v = 0$ and $D = 0$. If the number of nuclei n is

insufficient, satisfying the conditions following from Eq. (20),

$$\begin{aligned} n &< 1/(2n_x^2) \text{ for FID,} \\ n &< 1/(8n_x^2 n_z^2) \text{ for echo,} \end{aligned} \tag{23}$$

discord D will periodically be smaller than Eq. (8). At the same time, inequalities (23) can be considered as conditions for the magnetic field at a limited number of nuclei. When the magnetic field increases above the boundary value determined by inequalities (23), the achievable value of discord decreases because $n_x \longrightarrow 0$ (decrease for echo also occurs in the other limiting case of weak magnetic fields because $n_z \longrightarrow 0$ in this case).

Under certain conditions, which can be derived from Eqs. (20), $v = 1$ and, therefore, $U_0^2(t) = (1 - v)^2 = 0$. In this case, according to Eq. (17), $g(t) = 0$ and $|K| = 1$; consequently, mutual information $I(\rho)$ is maximal, whereas $D = 0$.

To physically explain these properties, we consider density matrix (3). According to Eq. (9), the imaginary part of the operator $\hat{U}^{+}_{(f,e)}$ contains the product of an odd number of operators $\hat{I}_{jx}$ and $\hat{I}_{jy}$, whereas the real part includes the product of an even number of these operators. Therefore, terms with the electron-spin operators $\hat{S}_y$ and $\hat{S}_x$ are responsible for different correlations. The quantum part of correlations is lost when density matrix (3) is projected on one direction at measurement (6). The exception is the case of one nucleus $n = 1$ in which all correlations are in the term of one direction $\hat{S}_y$. For this reason, projection on this direction is not accompanied by loss of correlations and quantum discord is zero (with the accuracy under consideration to the terms β_S^2, whereas higher-order terms are nonzero, as can be seen in the general solution for the two-qubit DQC1 model [23]). The term of one direction—$\hat{S}_x$ at even n values and $\hat{S}_y$ at odd n values—retains in Eq. (3) with operators (9) under the condition $U_0^2(t) = 0$. At $vn \ll 1$, the preferential y direction ($\hat{S}_y$) is conserved for correlations; consequently, discord (21) is small.

Finally, if $v \ll 1$, but $vn > 1$, discord (22) tends to the maximum value. The structure of this state can be analyzed using representation (C.3) in Appendix C for the density matrix in the basis of the eigenfunctions $|\Theta_k\rangle$ of evolution operators (4). This mixed state is represented in the form of the superposition of states with certain values of the evolution operator, which are in turn determined by the states of electron and nuclear spins. Each such state corresponds to a certain orientation of the electron spin vector $\langle \mathbf{S} \rangle_k$ in the xy plane. Owing to the condition $vn > 1$ at $v \ll 1$, the vectors $\langle \mathbf{S} \rangle_k$ are uniformly distributed over all directions. In this case, in Eq. (C.6),

$$2^{-n} \sum_k \cos^2(\varphi + \Theta_k) \approx 1/2, \tag{24}$$

and $\tau_{\mathrm{Re}} \approx \tau_{\mathrm{Im}} \approx 0$. Spin operators in different directions do not commute with each other and, consequently, cannot be measured simultaneously. Under condition (24), half the correlations are lost at projection (6) on any direction and quantum discord reaches the maximum according to Eq. (22). In this case, since the states under consideration are separable states, quantum entanglement characterizing quantum correlations of another type is absent [6–9, 17, 19, 21–23]. The analysis of the operation of the DQC1 computer shows that entanglement appears at low temperatures when $\beta_S > 1$ [17]. Under these conditions, the high-temperature approximation is inapplicable.

We return to the case of different hyperfine coupling constants in Eqs. (11)–(16). At small v_j values, vn in Eqs. (21) and (22) should be replaced by $\sum_j v_j$. When these parameters increase, the conditions $v_j = 1$ will be satisfied for different nuclei at different times; consequently, the common point $v = 1$, as well as the minimum of discord at it observed in the figure, will be absent. A quite uniform distribution of electron spins in the xy plane once appearing will further be conserved; therefore, achieving the maximum value, discord holds this value at large times.

Correlations can be measured without losses if the unlocking procedure for classical correlations proposed in [36] is used. To this end, the projective measurement of the nuclear system should be performed in the basis of the eigenfunctions $|\Theta_k\rangle\langle\Theta_k|$ of the evolution operator (see Appendix C). The use of this information at the measurement of the spin S makes it possible to choose the correct direction $\varphi_k = -\Theta_k$ in projector (6). To obtain complete information, the measurement should be performed for each Θ_k value, i.e., for each element of the ensemble of systems in different classical states. After that, the traces of matrices and mutual information can be calculated on a classical computer. Now,

$$2^{-n} \sum_k \cos^2(\varphi + \Theta_k) = 1$$

in Eq. (C.6) instead of 1/2 in Eq. (24). This means that such a measurement provides complete information. It should be emphasized that the trace of the evolution matrix is obtained in one measurement of $\langle \hat{S}_x \rangle$ or $\langle \hat{S}_y \rangle$ in the quantum system. In this case, quantum information unknown to an observer is summed on spin S. The summation of classical information known to the observer requires $N = 2^n$ operations of summation of matrix elements on a classical computer.

The above analysis obviously refers not only to particular conditions of spin echo, but also to other quantum systems, including the DQC1 model. To implement this model on a classical system (on the classical computer), an ensemble of $N = 2^n$ classical systems is required. One of the operations U_{ii}, $i = 1, \ldots, N$ is performed on each element of the ensemble. Then, these results are sequentially summed: $\sum_{i=1}^{N} U_{ii}$. In the case of the implementation on a quantum system (on a DQC1 quantum computer), a quantum superposition of $N = 2^n$ states is prepared and the operator $\hat{U}_n$ is applied on all states simultaneously. The results are summed on spin S "without reading" and only the final result is measured. Thereby, the advantage of the DQC1 quantum computer over the classical computer is possibly due to the indicated property of quantum information in a superposition state. This property of the quantum system (quantum information) is characterized by quantum discord, which is equal to locking classical correlation, as was shown in [37]. However, the relation is ambiguous because quantum calculations can be performed at zero discord [21].

Finally, as was mentioned in the Introduction, the capability of changing the state of the reservoir after a change in the state of the electron spin (back action) is used as a quantization characteristic of the reservoir of nuclear spins surrounding the electron spin. Such a change results in an incomplete recovery of echo and in a decrease in its amplitude $g_{(e)}(t)$. As a result, correlations appear between the electron and nuclear spins; these correlations are characterized by mutual information (12) expressed in terms of the echo amplitude squared. The features of the time and magnetic-field dependences of $g_{(e)}(t)$ described in [30] will be manifested in mutual information, which is accepted [8, 9] as a measure of total correlations. The quantum part of correlations is characterized by discord whose behavior was analyzed above (see figure). In particular, a decrease in ratio (21) with a decrease in parameter v (20) can be considered to a certain extent as the confirmation of the conclusion made in [30] about a decrease in quantization with an increase in the magnetic field, but the total amount of correlations decreases in this case. It is noteworthy that the authors of the cited work considered two-quantum transitions between levels with the spin projection +1 and −1 of the $S = 1$ spin in the NV center in diamond. After the replacement of A_{jx} by $2A_{jx}$, the above formulas obtained for $S = 1/2$, as well as the above conclusions followed from them about the behavior of quantum correlations, can be applied to this transition. However, they cannot be directly used for quantitative calculations because the conditions of the high-temperature approximation are violated for the electron spin of the NV center.

3. INCLUSION OF THE POLARIZATION OF NUCLEAR SPINS

The effect of the polarization of nuclear spins on discord is examined in this section. To this end, equilibrium density matrix (2) is supplemented by the term

$$\beta_I \Delta\hat{\rho}_{IS}/Z = \beta_I \sum_j \hat{I}_{jz}/Z.$$

The evolution of this part under the same conditions that Eqs. (3)–(10) can be represented in the form

$$\Delta\hat{\rho}_{IS}(t) = \sum_j \{ U_{j0}^{(f,e)}(t)\hat{I}_{jz} + \hat{S}_z\hat{I}_{jy}U_{jx}^{(f,e)}(t) + \hat{S}_z\hat{I}_{jx}U_{jy}^{(f,e)}(t) \}. \quad (25)$$

Thus, evolution transforms the multispin system under consideration to the state

$$\rho(t) = \{1 - \beta_S\Delta\hat{\rho}_{SI}(t) + \beta_I\Delta\hat{\rho}_{IS}(t)\}/Z. \quad (26)$$

Mutual information (5) for this state is found in the form (see Appendix B)

$$I(\rho) = \frac{1}{8\ln 2}\left[\beta_S^2\left(1 - \prod_j U_{j0}^2(t)\right) + \beta_I^2\sum_j (1 - U_{j0}^2)\right], \quad (27)$$

and mutual information of the state after the von Neumann measurement with projectors (6), where $a_z = \cos\theta$, $a_x = \sin\theta\cos\varphi$, and $a_y = \sin\theta\sin\varphi$, is given by the expression

$$I(\hat{\Pi}_S(\hat{\rho})) = \frac{1}{16\ln 2} \times \left\{ \beta_S^2\sin^2\theta\left[1 - \prod_j U_{j0}^2(t) - K\cos(2\varphi)\right] + 2\beta_I^2\cos^2\theta\sum_j (1 - U_{j0}^2) + 2\beta_I\beta_S\sin\varphi\sin\theta\cos\theta \times \sum_j (U_{jx}(t)U_{jy}(t))\prod_{k(\neq j)} U_{k0}(t)\right\}. \quad (28)$$

At small times, when $U_{j0}^2(t)$ is close to unity and has the form $U_{j0}^2(t) = (1 - v_j)^2$, where $v_j \ll 1$ is specified by Eqs. (20), the cross term in Eq. (28) can be neglected because, according to Eq. (10),

$$|U_{jx}(t)U_{jy}(t)| < 1 - U_{j0}^2(t) \approx 2v_j.$$

Then,

$$I(\hat{\Pi}_S(\hat{\rho}))8\ln 2 = [\beta_S^2(1 - \cos(2\varphi))\sin^2\theta + \beta_I^2\cos^2\theta]\sum_j v_j. \quad (29)$$

In the same approximation,

$$I(\hat{\rho}) = \frac{\beta_S^2+\beta_I^2}{4\ln 2}\sum_j v_j. \quad (30)$$

Function (29) reaches a maximum at $\varphi = \pi/2$. In this case,

$$I[\hat{\Pi}_S(\hat{\rho})]4\ln 2 = [\beta_S^2\sin^2\theta + \beta_I^2\cos^2\theta]\sum_j v_j.$$

This expression is maximal at $\theta = \pi/2$ if $\beta_S^2 > \beta_I^2$ and at $\theta = 0$ if $\beta_S^2 < \beta_I^2$. For this reason, discord (7) can be represented in the form

$$D = \begin{cases} \dfrac{\beta_I^2}{4\ln 2}\sum_j v_j = I(\rho)\dfrac{\beta_I^2}{\beta_S^2+\beta_I^2} \text{ at } \beta_S^2 > \beta_I^2, \\ \dfrac{\beta_S^2}{4\ln 2}\sum_j v_j = I(\rho)\dfrac{\beta_S^2}{\beta_S^2+\beta_I^2} \text{ at } \beta_S^2 < \beta_I^2. \end{cases} \quad (31)$$

It is noteworthy that higher powers of the time in the expansion, which leads to contribution (21), should be taken into account at very small β_I^2 values.

Under other conditions at quite large times for a sufficiently large number of nuclei, when all products with respect to j in Eqs. (27) and (28) can be approximated by zero, $K = 0$ and the dependence on the angle φ disappears in Eq. (28):

$$I(\hat{\Pi}_S(\hat{\rho})) = \frac{1}{16\ln 2}\left\{\beta_S^2\sin^2\theta + 2\beta_I^2\sin^2\theta\sum_j(1-U_{j0}^2)\right\}. \quad (32)$$

Function (32) is maximal at $\theta = \pi/2$ if

$$\beta_S^2 > 2\beta_I^2\sum_j(1-U_{j0}^2),$$

and at $\theta = 0$ if

$$\beta_S^2 < 2\beta_I^2\sum_j(1-U_{j0}^2).$$

In the former case,

$$D \approx \frac{1}{8\ln 2}\left\{\frac{\beta_S^2}{2} + \beta_I^2\sum_j(1-U_{j0}^2)\right\}, \quad (33)$$

whereas in the latter case,

$$D \approx \frac{\beta_S^2}{8\ln 2}. \quad (34)$$

We compare these expressions to the results obtained in the preceding section. When the polarization of nuclear spins is taken into account, additional terms appear in $I(\rho)$ and D. As a result, the behavior at small times changes: $D/I(\rho)$ tends to finite value (31) rather than to zero as would be according to (21). This ratio increases at large times, as follows from the comparison of Eqs. (33) and (22). Finally, because of the additional term $\Delta\hat{\rho}_{IS}(t)$ given by Eq. (25), which does not commute with $\Delta\hat{\rho}_{SI}(t)$, the result of the von Neumann measurement on nuclear spins changes. Now, projector (C.2) composed of the eigenfunctions of the unitary operator $\hat{U}^{\pm}_{(f,e)}$ given by Eq. (4) changes the state $\rho(t)$ specified by Eq. (26); consequently, discord at the measurement on nuclear spins will be nonzero.

There is another approach to the analysis of correlations in the multispin system. This approach involves the reduction of density matrix (26) to the density matrix of a pair of spins [9, 38]. We calculate the trace over the spin variables of all nuclear spins except for the jth spin of the environment. As a result, the reduced density matrix of the two-spin system is obtained in the form

$$\hat{\rho}_{Sj}(t) = \frac{1}{4}\{1 + U_0[-\beta_S(t)\hat{S}_x + \beta_I\hat{I}_{jz}] + \beta_I\hat{S}_z[U_x\hat{I}_{jy} + U_y\hat{I}_{jx}] + \beta_S(t)\hat{S}_y[U_y\hat{I}_{jy} + U_x\hat{I}_{jx}]\}. \quad (35)$$

To simplify the formulas, the following notation was introduced:

$$\beta_S(t) = \beta_S\prod_{k(\neq j)}U_{k0}^{(f,e)}(t), \quad U_0 = U_{j0}^{(f,e)}(t), \quad U_x = U_{jx}^{(f,e)}(t), \quad U_y = U_{jy}^{(f,e)}(t). \quad (36)$$

After the cyclic change of spin variables $(\hat{S}_x, \hat{S}_y, \hat{S}_z)$ to $(\hat{S}_z, \hat{S}_x, \hat{S}_y)$, state (35) acquires the form of the X state [9, 38]. Discord remains the same after such a change. Discord for the X state was calculated in many works. Instead of the analysis of complicated formulas obtained in those works, it seems more reasonable to obtain the result directly for our simple model in the high-temperature approximation.

The mutual information of state (35) is obtained in the form

$$I(\hat{\rho}_{Sj}(t)) = \frac{1}{8\ln 2}(1-U_0^2)(\beta_S^2(t)+\beta_I^2). \quad (37)$$

In order to separate the classical part of correlations, the orthogonal measurement with projectors (6) for density matrix (35) is performed. The operator S_x enters into this matrix separately from the nuclear spin operator and, consequently, does not contribute to mutual information both before measurements and after them. Since $I(\hat{\Pi}_S(\hat{\rho}_{Sj}(t)))$ is independent of a_x, to reach the maximum value, the sum of the squares of two other direction cosines should be maximal, which

is achieved at $a_x = 0$, $a_z = \cos\varphi$, and $a_y = \sin\varphi$. As a result,

$$I(\hat{\Pi}_S(\hat{\rho}_{Sj}(t))) = \frac{1}{16\ln 2}\{(1-U_0^2)(\beta_S^2(t)+\beta_I^2) - \cos(2\varphi)(1-U_0^2)(\beta_S^2(t)-\beta_I^2) + \sin(2\varphi)\beta_S(t)\beta_I U_x U_y\}. \quad (38)$$

The classical part of correlations can be separated by another method of orthogonal measurements of the nuclear spin by means of the projectors

$$\hat{\Pi}_{I\pm} = \frac{1}{2} \pm (b_x\hat{I}_{jx} + b_y\hat{I}_{jy} + b_z\hat{I}_{jx}),$$

where b_α are the direction cosines. We take $b_z = 0$, $b_y = \cos\psi$, and $b_x = \sin\psi$, because the operator I_{jz} appears in matrix (35) separately from the electron spin operator and $I(\hat{\Pi}_I(\hat{\rho}_{Sj}(t)))$ does not contain a contribution with b_z. In this case,

$$I(\hat{\Pi}_I(\hat{\rho}_{Sj}(t))) = \frac{1}{32\ln 2}\Big\{(\beta_S^2(t)+\beta_I^2) \times [2(1-U_0^2) + \sin(2\psi)U_xU_y] + \frac{1}{2}\cos(2\psi)(U_y^2-U_x^2)(\beta_S^2(t)-\beta_I^2)\Big\}. \quad (39)$$

The desired amount of classical correlations is found after the determination of the maxima of functions (38) and (39) in the angles φ and ψ, respectively. From the condition of maximum of Eqs. (38) and (39), we obtain the equations

$$\tan(2\varphi) = -\frac{U_xU_y\beta_I\beta_S(t)}{(1-U_0^2)(\beta_S^2(t)-\beta_I^2)},$$

and

$$\tan(2\psi) = \frac{2U_xU_y(\beta_S^2(t)+\beta_I^2)}{(U_x^2-U_y^2)(\beta_S^2(t)-\beta_I^2)}.$$

respectively.

Quantum discord D_j is determined by Eq. (7) after the subtraction of classical correlations from total correlations (37). At $\beta_I = 0$ (or $\beta_S = 0$), $D_j = 0$. Discord D_j at nonzero polarizations is nonzero at measurements both in S and in I. In particular, at $\beta_S^2(t) = \beta_I^2 = \beta^2$, we obtain

$$D_j = \frac{\beta^2}{16\ln 2}\{2(1-U_0^2) - |U_xU_y|\}. \quad (40)$$

Discord at other values of the parameters can be calculated numerically by the resulting formulas.

It is noteworthy that the ratio $D_j/I(\hat{\rho}_{Sj}(t))$ at small times is specified by Eq. (31) with the replacement of β_S^2 by $\beta_S^2(t)$. In this case, discords in two cases are different, because mutual information (30) in the case of total density matrix (26) is the sum of the amounts of mutual information for all pairs represented by reduced matrices (35).

Thus, it has been shown that the method of reduction of the density matrix to a two-spin electron–nuclear system provides a qualitatively correct description of pair correlations and dynamics of their quantum and classical parts. Such correlations play the main role at $\beta_S \approx \beta_I$ and small times. Multispin correlations become dominant at large times. Pair correlations decay, which is manifested in a decrease in $\beta_S(t)$ (36) in the results obtained for the reduced density matrix. In this case, mutual information contains a term proportional to β_I^2, which does not include quantum correlations. On the contrary, mutual information (27), as well as discord given by Eq. (33) and (34), is maximal when all correlations are completely taken into account.

4. CONCLUSIONS

The dynamics of the system of an electron spin surrounded by nuclear spins under the conditions of free-precession decay and electron spin echo has been studied. The damping of the observed signals is attributed to the formation of correlations between electron and nuclear spins. In the central-spin and high-temperature approximations, the density matrix is represented in the form of the sum of terms with different numbers of nuclear spin operators responsible for different correlations. Under the conditions of the FID and spin echo, the same combinations of spin operators appear, where the dependences of the coefficients on the time and magnetic field are different for these two cases. Some of these terms disappear after the projection on an orthogonal basis. Mutual information calculated over all the terms of the density matrix specifies the magnitude of total correlations, whereas mutual information calculated over the terms remaining after projection gives the magnitude of classical correlations. Their difference determines the magnitude of quantum correlations characterized by discord. At the present time, the quantum properties of the system under consideration are studied in the FID signals and a decrease in the spin echo amplitude, which are determined by terms with one spin operator. There are more complex methods for measuring terms with a large number of spin operators. In particular, two-spin terms in the density matrix were measured in [29] with the use of the quantum state tomography method, while authors of [24] proposed to use multiquantum NMR spectroscopy to measure terms with a large number of spin operators. The inclusion of multispin terms of the density matrix will allow finer studies of the quantum properties of the electron–nuclear system.

APPENDIX A

EVOLUTION OPERATOR

The properties of raising and lowering operators allow the following transformations of the evolution operators of the FID and spin echo:

$$\begin{aligned}\exp(-it\hat{H})S_+\exp(it\hat{H}) &= \exp(-it\hat{H}_+)\\ &\times \exp(-it\hat{H}_-)\hat{S}_+ \equiv \hat{U}_f^+(t)\hat{S}_+,\\ \exp(-it\hat{H})\hat{P}_{180}&\exp(-it\hat{H})\hat{S}_-\\ &\times \exp(it\hat{H})\hat{P}_{180}\exp(it\hat{H})\\ &= \exp(-it\hat{H}_+)\exp(-it\hat{H}_-)\\ &\times \exp(it\hat{H}_+)\exp(-it\hat{H}_-)\hat{S}_+\\ = \exp(-it\hat{H}_+)\hat{U}_f^-(t)&\exp(it\hat{H}_-)\hat{S}_+ \equiv \hat{U}_e^+(t)\hat{S}_+,\end{aligned} \tag{A.1}$$

where $\hat{P}_{180}$ is the rotation operator of the spin S by 180° about the x axis of the rotating reference frame.

In the case $\hat{H}_{II} = 0$, the operators given by Eqs. (4) for different nuclear spins commute with each other; as a result, the product of their contributions appears in Eq. (9). We consider the contribution from the interaction with one nuclear spin. The properties of the Pauli matrices allow the following transformation of exponential operators:

$$\begin{aligned}&\exp(-it\Omega n_x\hat{I}_x - it\Omega n_z\hat{I}_z)\\ &= \cos(\Omega t/2)\hat{E}_2 - i2\sin(\Omega t/2)\{n_x\hat{I}_x + n_z\hat{I}_z\},\end{aligned} \tag{A.2}$$

where $\hat{E}_2$ is the identity matrix. Successively applying this formula to operators in Eqs. (4) and performing necessary transformations, we obtain Eqs. (9) and (10). Since the evolution operators are unitary, the coefficients satisfy the relation

$$\begin{aligned}&\hat{U}^+_{j(f,e)}(t)\hat{U}^-_{j(f,e)}(t)\\ &= \{U^{(f,e)}_{j0}(t) + i\hat{I}_{jx}U^{(f,e)}_{jx}(t) + i\hat{I}_{jy}U^{(f,e)}_{jy}(t)\}\\ &\times \{U^{(f,e)}_{j0}(t) - i\hat{I}_{jx}U^{(f,e)}_{jx}(t) - i\hat{I}_{jy}U^{(f,e)}_{jy}(t)\}\\ &= (U^{(f,e)}_{j0}(t))^2 + \frac{(U^{(f,e)}_{jx}(t))^2}{4} + \frac{(U^{(f,e)}_{jy}(t))^2}{4} = 1.\end{aligned} \tag{A.3}$$

APPENDIX B

CALCULATION OF MUTUAL INFORMATION

For density matrix (3), we find the reduced matrices

$$\begin{aligned}\hat{\rho}_I(t) &= \mathrm{Tr}_S\hat{\rho}(t) = \frac{2\hat{E}_I}{Z},\\ \hat{\rho}_S(t) &= \mathrm{Tr}_I\hat{\rho}(t)\\ &= \frac{1}{2}\left[\hat{E}_S - \frac{\beta_S}{2}\{\hat{S}_+\tau_+(t) + \hat{S}_-\tau_-(t)\}\right],\end{aligned} \tag{B.1}$$

where

$$\tau_\pm(t) = \frac{1}{2^n}\mathrm{Tr}_I\hat{U}^\pm_{(f,e)}(t),$$

and $\hat{E}_I$ and $\hat{E}_S$ are the identity matrices. In the high-temperature approximation, the density matrices of interest have the form

$$\hat{\rho} = \frac{1}{Z}[1 \pm \beta\Delta\hat{\rho}].$$

In the lowest order in the inverse temperature, the von Neumann entropy is given by the expression [33, 34]

$$S(\hat{\rho}) = -\mathrm{Tr}\{\hat{\rho}\log_2\hat{\rho}\} = \log_2 Z - \frac{\beta^2}{2Z\ln 2}\mathrm{Tr}(\Delta\hat{\rho})^2. \tag{B.2}$$

In this approximation, the following expression is obtained for mutual information (5):

$$\begin{aligned}I(\hat{\rho}) = \frac{\beta_S^2}{2\ln 2}&\left\{\frac{1}{Z}\mathrm{Tr}(\Delta\hat{\rho}_{SI})^2 - \frac{1}{2}\mathrm{Tr}_S(\Delta\hat{\rho}_S)^2\right.\\ &\left. - \frac{1}{2^n}\mathrm{Tr}_I(\Delta\hat{\rho}_I)^2\right\} = \frac{\beta_S^2}{8\ln 2}[1 - \tau_+(t)\tau_-(t)],\end{aligned} \tag{B.3}$$

which for system (9) gives Eq. (12).

Performing projection of matrix (3) with the use of projectors (6) by the formula

$$\begin{aligned}\hat{\Pi}_S(\Delta\hat{\rho}_{SI}(t)) = \sum_{m=\pm}&(\hat{\Pi}_{Sm}\otimes\hat{E}_I)\\ &\times\Delta\hat{\rho}_{SI}(t)(\hat{\Pi}_{Sm}\otimes\hat{E}_I),\end{aligned}$$

we obtain

$$\begin{aligned}\hat{\Pi}_S(\Delta\hat{\rho}_{SI}(t)) &= \frac{1}{4}\hat{\Pi}_{S+}\{a_x(\hat{U}^+_{(f,e)}(t) + \hat{U}^-_{(f,e)}(t))\\ &+ ia_y(\hat{U}^+_{(f,e)}(t) - \hat{U}^-_{(f,e)}(t))\}\\ &- \frac{1}{4}\hat{\Pi}_{S-}\{a_x(\hat{U}^+_{(f,e)}(t) + \hat{U}^-_{(f,e)}(t))\\ &+ ia_y(\hat{U}^+_{(f,e)}(t) - \hat{U}^-_{(f,e)}(t))\}.\end{aligned} \tag{B.4}$$

In the lowest order in the inverse temperature, the mutual information for matrix (B.4) is given by the expression

$$\begin{aligned}I(\hat{\Pi}_S(\hat{\rho})) &= S(\hat{\Pi}_S(\hat{\rho}_S)) + S(\hat{\Pi}_S(\hat{\rho}_I))\\ &- S(\hat{\Pi}_S(\hat{\rho})) = \frac{\beta_S^2}{2\ln 2}\left\{\frac{1}{Z}\mathrm{Tr}(\hat{\Pi}_S(\Delta\hat{\rho}_{SI}))^2\right.\\ &\left. - \frac{1}{2}\mathrm{Tr}_S(\hat{\Pi}_S(\Delta\hat{\rho}_S))^2 - \frac{1}{2^n}\mathrm{Tr}_I(\Delta\rho_I)^2\right\}.\end{aligned} \tag{B.5}$$

Here,

$$\begin{aligned}
&\mathrm{Tr}_I(\Pi_S\Delta\hat{\rho}_I)^2 = \mathrm{Tr}_I(\Delta\hat{\rho}_I)^2 = 0,\\
&\mathrm{Tr}_S(\hat{\Pi}_S(\Delta\hat{\rho}_S))^2 = \frac{(a_x\tau_{\mathrm{Re}} - a_y\tau_{\mathrm{Im}})^2}{2},\\
&\frac{1}{Z}\mathrm{Tr}(\hat{\Pi}_S(\Delta\hat{\rho}_{SI}))^2 \qquad\qquad (B.6)\\
&= \frac{1}{2^{n+4}}\mathrm{Tr}_I\{a_x(\hat{U}^+_{(f,e)}(t) + \hat{U}^-_{(f,e)}(t))\\
&\quad + ia_y(\hat{U}^+_{(f,e)}(t) - \hat{U}^-_{(f,e)}(t))\}^2,
\end{aligned}$$

where τ_{Re} and τ_{Im} are the real and imaginary parts of $\tau_\pm$, respectively. For system (9), $\tau_{\mathrm{Im}} = 0$ and it follows from Eqs. (B.6) that

$$\begin{aligned}
&2\mathrm{Tr}_S(\hat{\Pi}_S(\Delta\hat{\rho}_S))^2 = (\tau_{\mathrm{Re}}a_x)^2 = a_x^2\prod_j U_{j0}^2(t),\\
&\frac{8}{Z}\mathrm{Tr}(\hat{\Pi}_S(\Delta\hat{\rho}_{SI}))^2 = (a_x^2 + a_y^2) + (a_x^2 - a_y^2)\\
&\quad\times\prod_j\left\{U_{j0}^2(t) - \frac{1}{4}U_{jx}^2(t) - \frac{1}{4}U_{jy}^2(t)\right\} \qquad (B.7)\\
&= (a_x^2 + a_y^2) + (a_x^2 - a_y^2)\prod_j\{2U_{j0}^2(t) - 1\},
\end{aligned}$$

where property (A.3) is used in the last equality. The substitution of Eqs. (B.7) into Eq. (B.5) gives either Eq. (13) or the corresponding contribution in Eq. (28) depending on the choice of the direction cosines indicated in the text.

Similar calculations can be performed for contribution (25) from nuclei. First, calculating the reduced matrices in this state

$$\begin{aligned}
&\mathrm{Tr}_I\hat{\rho}_{IS}(t) = 0,\\
&\Delta\hat{\rho}_I(t) = \mathrm{Tr}_S\hat{\rho}_{IS}(t) = \sum_j\hat{I}_{jz}U_{j0}(t)
\end{aligned}$$

and the von Neumann entropy taking into account that

$$\begin{aligned}
&\mathrm{Tr}\{\hat{\rho}(t)\log_2\hat{\rho}(t)\} = \mathrm{Tr}\{\hat{\rho}(0)\log_2\hat{\rho}(0)\}\\
&= \frac{\beta_S^2 + n\beta_I^2}{8\ln 2} - (n+1),
\end{aligned}$$

we obtain Eq. (27). Second, the orthogonal von Neumann measurement with projectors (6) gives

$$\begin{aligned}
&\hat{\Pi}_S(\Delta\hat{\rho}_{IS}(t)) = \sum_j\{U_{j0}^{(f,e)}(t)\hat{I}_{jz}\}\\
&+ \frac{1}{2}\hat{\Pi}_{S+}a_z\sum_j\{\hat{I}_{jy}U_{jx}^{(f,e)}(t) + \hat{I}_{jx}U_{jy}^{(f,e)}(t)\}\\
&- \frac{1}{2}\hat{\Pi}_{S-}a_z\sum_j\{\hat{I}_{jy}U_{jx}^{(f,e)}(t) + \hat{I}_{jx}U_{jy}^{(f,e)}(t)\}
\end{aligned}$$

and the corresponding contribution in Eq. (28) by formula (B.5) rewritten for this case.

APPENDIX C

CALCULATION IN THE ORTHOGONAL BASIS OF THE NUCLEAR SYSTEM

We introduce the basis $|\Theta_k\rangle$ consisting of the $N = 2^n$ eigenfunctions of evolution operators (4)

$$\hat{U}^\pm_{(f,e)}|\Theta_k\rangle = \exp(\pm i\Theta_k)|\Theta_k\rangle \qquad (C.1)$$

and projection operators on these states

$$\hat{\Pi}_k = |\Theta_k\rangle\langle\Theta_k|. \qquad (C.2)$$

Density matrix (3) in this representation has the form

$$\begin{aligned}
\hat{\rho}(t) &= \frac{1}{Z}\left\{1 - \frac{\beta_S}{2}\sum_k[\hat{S}_+\exp(i\Theta_k)\right.\\
&\quad\left. + \hat{S}_-\exp(-i\Theta_k)]\otimes|\Theta_k\rangle\langle\Theta_k|\right\} \qquad (C.3)\\
&= \frac{1}{Z}\left\{1 - \beta_S\sum_k[\hat{S}_x\cos\Theta_k - \hat{S}_y\sin\Theta_k]\otimes|\Theta_k\rangle\langle\Theta_k|\right\}.
\end{aligned}$$

Mutual information is given by Eq. (B.3), where

$$\tau_\pm(t) = \frac{1}{2^n}\sum_k\exp(\pm i\Theta_k). \qquad (C.4)$$

The projection of matrix (C.3) by means of projectors (6) with $a_z = 0$, $a_x = \cos\varphi$, and $a_y = \sin\varphi$ gives

$$\begin{aligned}
\hat{\Pi}_S(\Delta\hat{\rho}_{SI}(t)) &= \frac{1}{2}\sum_k\{\hat{\Pi}_{S+}\cos(\varphi + \Theta_k)\otimes|\Theta_k\rangle\langle\Theta_k|\\
&\quad - \hat{\Pi}_{S-}\cos(\varphi + \Theta_k)\otimes|\Theta_k\rangle\langle\Theta_k|\}. \qquad (C.5)
\end{aligned}$$

In this case,

$$\frac{1}{Z}\mathrm{Tr}(\hat{\Pi}_S(\Delta\hat{\rho}_{SI}))^2 = \frac{1}{2^{n+2}}\sum_k\cos^2(\varphi + \Theta_k)$$

and Eq. (B.5) yields

$$I(\hat{\Pi}_S(\hat{\rho})) = \frac{\beta_S^2}{8\ln 2}\left\{\frac{1}{2^n}\sum_k \cos^2(\varphi + \Theta_k) - (\tau_{\mathrm{Re}}\cos\varphi - \tau_{\mathrm{Im}}\sin\varphi)^2\right\}. \quad \text{(C.6)}$$

It is noteworthy that, for model (9),

$$\exp(i\Theta_k) = \prod_j \exp(i\Theta_k^j),$$

where Θ_k^j at various k values can be either $2\arcsin\sqrt{v_j/2}$ and $-2\arcsin\sqrt{v_j/2}$.

REFERENCES

1. E. L. Hahn, Phys. Rev. **80**, 580 (1950).
2. K. M. Salikhov, A. G. Semenov, and Yu. D. Tsvetkov, *Electron Spin Echo and Its Applications* (Nauka, Novosibirsk, 1976) [in Russian].
3. B. Blyumikh, *Principles of Nuclear Magnetic Resonance* (Tekhnosfera, Moscow, 2007) [in Russian].
4. J. Waugh, *New NMR Methods in Solid State Physics* (Cambridge University Press, Cambridge, 1976; Mir, Moscow, 1978).
5. R. A. Jalabert and H. M. Pastawski, Phys. Rev. Lett. **86**, 2490 (2001).
6. K. A. Valiev and A. A. Kokin, *Quantum Computers: Hopes and Reality* (Regular and Chaotic Dynamics, Moscow, 2001) [in Russian].
7. M. A. Nielsen and I. L. Chuang, *Quantum Computation and Quantum Information* (Cambridge University Press, Cambridge, 2000; Mir, Moscow, 2006).
8. J. Preskill, *Quantum Information and Computation* (California Institute of Technology, Pasadena, California, United States, 1998; Regular and Chaotic Dynamics, Moscow, 2008–2011).
9. K. Modi, A. Brodutch, H. Cable, T. Paterek, and V. Vedral, Rev. Mod. Phys. **84**, 1655 (2012).
10. G. G. Kozlov, J. Exp. Theor. Phys. **105** (4), 803 (2007).
11. W. M. Witzel, M. S. Carroll, L. Cywinski, and S. D. Sarma, Phys. Rev. B: Condens. Matter **86**, 035452 (2012).
12. Nan Zhao, Sai-Wah Ho, and Ren-Bao Liu, Phys. Rev. B: Condens. Matter **85**, 115303 (2012).
13. L. T. Hall, J. H. Cole, and L. C. L. Hollenberg, arXiv:1309.5921.
14. J. Hackmann and F. B. Anders, Phys. Rev. B: Condens. Matter **89**, 045317 (2014).
15. J. J. L. Morton and B. W. Lovett, Annu. Rev. Condens. Matter Phys. **2**, 189 (2011).
16. E. Knill and R. Laflamme, Phys. Rev. Lett. **81**, 5672 (1998).
17. A. Datta, A. Shaji, and C. M. Caves, Phys. Rev. Lett. **100**, 050502 (2008).
18. A. F. Fahmy, R. Max, W. Bermel, and S. J. Glasser, Phys. Rev. A: At., Mol., Opt. Phys. **78**, 022317 (2008).
19. S. Wu, U. V. Poulsen, and K. Molmer, Phys. Rev. A: At., Mol., Opt. Phys. **80**, 032319 (2009).
20. G. Passante, O. Moussa, C. A. Ryan, and R. Laflamme, Phys. Rev. Lett. **103**, 250501 (2009).
21. B. Dakic, V. Vedral, and C. Brukner, Phys. Rev. Lett. **105**, 190502 (2010).
22. A. Datta and A. Shaji, Int. J. Quantum Inf. **9**, 1787 (2011).
23. G. Passante, O. Moussa, and R. Laflamme, Phys. Rev. A: At., Mol., Opt. Phys. **85**, 032325 (2012).
24. M. Mehring and J. Mende, Phys. Rev. A: At., Mol., Opt. Phys. **73**, 052303 (2006).
25. T. Morimae, K. Fujii, and J. F. Fitzsimons, Phys. Rev. Lett. **112**, 130502 (2014).
26. E. I. Kuznetsova and A. I. Zenchuk, Phys. Lett. A **376**, 1029 (2012).
27. A. Y. Chernyavskiy, S. I. Doronin, and E. B. Fel'dman, Phys. Scr., **T160**, 014007 (2014).
28. V. E. Zobov, Theor. Math. Phys. **177** (1), 1377 (2013).
29. X. Rong, F. Jin, and Z. Wang, Phys. Rev. B: Condens. Matter **88**, 054419 (2013).
30. F. Reinhard, F. Shi, N. Zhao, F. Rempp, B. Naydenov, J. Meijer, L. T. Hall, L. Hollenberg, J. Du, R.-B. Liu, and J. Wrachtrup, Phys. Rev. Lett. **108**, 200402 (2012).
31. A. Laraoui, F. Dolde, C. Burk, F. Reinhard, J. Wrachtrup, and C. A. Meriles, Nat. Commun. **4**, 1651 (2013).
32. T. Fink and H. Bluhm, arXiv:1402.0235.
33. A. Abragam and M. Goldman, *Nuclear Magnetism: Order and Disorder* (Clarendon, Oxford, 1982; Mir, Moscow, 1984).
34. R. Auccaise, L. C. Celeri, D. O. Soares-Pinto, E. R. deAzevedo, J. Maziero, A. M. Souza, T. J. Bonagamba, R. S. Sarthour, I. S. Oliveira, and R. M. Serra, Phys. Rev. Lett. **107**, 140403 (2011).
35. F. Galve, G. L. Giorgi, and R. Zambrini, Europhys. Lett. **96**, 40005 (2011).
36. D. P. DiVincenzo, M. Horodecki, D. W. Leung, J. A. Smolin, and B. M. Terhal, Phys. Rev. Lett. **92**, 067902 (2004).
37. S. Boixo, L. Aolita, D. Cavalcanti, K. Modi, M. Piani, and A. Winter, Int. J. Quantum Inf. 9, 1643 (2011).
38. E. B. Fel'dman, E. I. Kuznetsova, and M. A. Yurishchev, J. Phys. A: Math. Theor. **45**, 475304 (2012).

Translated by R. Tyapaev